

# Characterizing Electric Field Distribution Due to Upward Initiated Lightning Around the Blades of a Rotating Wind Turbine

Godson I. Ikhazuangbe<sup>1</sup>, Mumtaj Begam<sup>1</sup>, Shahram Mohanna<sup>2</sup>, Promise T. Arole<sup>3</sup>, Iloayira Wariboko<sup>4</sup>, Osawaru N. Osarimwian<sup>5</sup>, Phillip Kpae<sup>6</sup>, Evbogbai Edekin<sup>7</sup>, Dikio Idoniboyeobu<sup>8</sup>

\*kecx4iga@nottingham.edu.my, godson2003@yahoo.com

<sup>1</sup>Department of Electrical and Electronic Engineering, The University of Nottingham Malaysia Campus, 43500, Semenyih, Selangor, Malaysia

<sup>2</sup>Faculty of Electrical and Computer Engineering, University of Sistan and Baluchestan, Daneshgah Road Zahedan, Iran.

<sup>3</sup>Faculty of Engineering, Enugu State University of Science and Technology, Nigeria.

<sup>4</sup>Captain Elechi Amadi Polytechnic Portharcourt, Nigeria.

<sup>5</sup>Ambrose Alli University, Department of Electrical/Electronic Engineering, PMB 14, Ekpoma, Edo State, Nigeria.

<sup>6</sup>Department of Electrical and Electronic Engineering, Kenule Beeson Sarowiwa Polytechnic Bori, Rivers State, Nigeria

<sup>7</sup>Department of Electrical and Electronic Engineering, Edo University Iyamho, Edo State, Nigeria

<sup>8</sup>Department of Electrical and Electronic Engineering, Rivers State University Portharcourt, Nigeria

**Abstract**— lightning constitutes the greatest threat to wind power industry. The characteristics of the distributed electric field prior to lightning strike plays an important role in determining lightning discharge attachment point as well as the efficiency of wind turbine protection systems. It was assumed that electric field due to upward initiated lightning might be the same as that of downward initiated lightning. However, more lightning damages which are upward initiated are now highly recorded. In this paper, the blades of a modern sized wind turbine (Vestas V100 with 2 MW rated power, 100 m rotor diameter, and 49 m long blade) are rotated from 0 to 360 degrees and used to investigate the characteristics of the distributed electric field around an operational wind turbine. The model of the extended vertical tri-pole cloud charge distribution model developed with finite element analysis is used to study the variations in maximum electric field strength required for the initiation of upward leader. By comparing the electric field strength as the blade is rotated, the field behavior is evaluated. In addition, experimental evaluations are carried out to support the findings. Result showed that the field around the blade surface and the receptor for an upward initiated lightning is more complex than was assumed and different from downward initiated lightning. This will consequently affect the proficiency of the protection device.

Keywords: FEM; lightning; protection; receptor; wind turbine.

## 1. INTRODUCTION

Modern wind turbines have become more prone to lightning strike due to their ever-increasing height. Field survey has shown that the number of lightning strikes grows as the turbine height increases. Lightning to modern tall wind turbines are majorly upward initiated and lightning to shorter wind turbines are majorly downward initiated. Upward lightning flashes have been observed to incept or initiate from tall towers (Diendorfer 2011), in America, in Japan (Wang, Takagi et al. 2008, Lu, Wang et al. 2009), in Europe (Miki, Rakov et al. 2005, Diendorfer, Pichler et al. 2009, Zhou, Diendorfer et al. 2012), and has been observed to be dominant at the Gaisberg Tower (Zhou, Diendorfer et al.

2012). Upward lightning flashes has also been reported to be triggered (Lyons, Nelson et al.) by wind turbines (Rachidi, Rubinstein et al. 2008, Wang, Takagi et al. 2008, Montanyà, Velde et al. 2014). An assessment of currents of upward lightning that were measured in tropical regions was presented in (Guimarães, Araujo et al. 2014).

The lightning strike incidence to wind turbine is generally evaluated based on probability of downward lightning attachment and does not account for upward flashes. However, in the presence of a thundercloud, tall wind turbines are increasingly subjected to upward lightning attachment self-triggered by the wind turbine, this can significantly increase the number of lightning strike to a wind turbine per annual (Diendorfer 2015), and is considered to be the main mechanism of lightning damages (Rachidi, Rubinstein et al. 2008). Alex Byrne and Matthew Malkin (Byrne and Malkin), discussed wind turbine lightning protection system's field performance assessment and suggested that increased risk for investments and insurance premiums in wind industry is due to poorly understood interaction of lightning and wind turbines. Also, the IEC 61400-24 approach to lightning damage risk assessment focuses more on downward lightning, and less on upward lightning. The design limits provided in IEC 61400-24 are for downward initiated lightning only, whereas, upward lightning has been found to have different characteristics than downward lightning (Diendorfer 2010, Diendorfer, Zhou et al. 2011). Also, upward leader's physical properties in nature have been found to be unlike those of leaders in the laboratory (Becerra and Cooray 2006, Becerra and Cooray 2008). Fundamentally, lightning attachment process of downward lightning are different to those of upward lightning, and as result, likely point of upward lightning attachments are uncertain. This is a major problem for modern wind turbine because lightning protection systems, the Electro Geometric Model (EGM) methods currently in use were designed considering downward lightning. In other words, existing protection systems are designed considering downward initiated lightning, these protection systems might not be effective for upward lightning. According to a paper by Vidyadhar Peesapati and Ian Cotton (Peesapati and Cotton 2009);

Existing turbine lightning protection systems have been shown reasonably effective for downward initiated lightning but there is an underlying risk in assuming the same systems will work for upward initiated lightning (Peesapati and Cotton 2009).

The efficiency of a lightning protection systems depends on the proper placement of the air-terminal which in turn depends on the understanding of the distributed electric field. This imply that the behavior of electric field distribution around a wind turbine is pertinent to the design of the lightning protection system.

Electric field due to downward initiated lightning has been investigated in literature, however up till now, the nature and properties of upward initiated lightning and how they affect the proficiency of the protection device has not been considered. Incidences of lightning damages which are upward initiated are highly reported recently.

Therefore, understanding the characteristics of the distributed electric field prior to upward initiated lightning strike is necessary in the design of modern efficient protection devices. In this paper, the blades of a modern sized wind turbine (Vestas V100 with 2 MW rated power, 100 m rotor diameter, and 49 m long blade) are rotated from 0 to 360 degrees and used to investigate the characteristics of the distributed electric field due to upward initiated lightning around an operational wind turbine protected with a tip receptor. The same concept of evaluation methodology that have been published in (Godson, Begam et al. 2017, Godson, Begam et al. 2017, Ikhazuangbe, Begam et al. 2019, Ikhazuangbe, Begam et al. 2019, Ikhazuangbe, Begam et al. 2019) are utilized. The simulation is done with COMSOL

Multiphysics software and it is considered that the magnitude of the electric field strength distributed on the wind turbine model determines the point of upward leader inception, it is also considered that the proficiency of the protection systems depends on the value of the distributed electric field, i.e., larger the electric field strength on the receptor and lower on the blade surface, the higher the proficiency of the receptor. By comparing the electric field strength as the blade is rotated, the electric field due to upward initiated lightning is characterized. In addition, experimental evaluations are carried out and the predicted lightning attachment locations on the blade surfaces are qualitatively compared with result from the numerical approach. The results are very important in the future development and design of efficient lightning protection systems. The rest of the paper is organized as follows: Section 2 deals with thundercloud and wind turbine model design, while Section 3 contains results and discussion on simulation, Section 4 deals with experimental evaluation and Section 5 deals with results and discussion on experimental evaluation, Section 6 finally concludes the paper.

## 2. THUNDERCLOUD AND WIND TURBINE MODEL

Lightning attachment to wind turbines has gained attention, with many research works focused on downward propagating lightning. Nevertheless, a few work, done on upward propagating lightning (Particularly due to electric fields from winter clouds developed at lower altitudes) has shown that apart from the fact that tall wind turbine can increase the number of lightning strike, due to rotation, turbines are triggering their own lightning (Rachidi, Rubinstein et al. 2008, Wang, Takagi et al. 2008, Montanyà, Velde et al. 2014), indicating that large portion of the lightning that attach to a wind turbine are upward initiated.

Upward lightning flashes are initiated from the enhancement of the electric field produced by thundercloud charge or close lightning discharges (Wang, Takagi et al. 2008, Zhou, Diendorfer et al. 2012). The critical ambient electric field also known as the stabilization electric field for the initiation of stable upward leaders from wind turbines produced during thunderstorms consists of two main components; (a) The slow increasing component  $E_{\text{cloud}}$  due to the charging process of thunderclouds and (b) The fast electric field change component  $\Delta E_{\text{cloud}}$ . Upward leaders in self-initiated upward lightning are majorly influenced by the slowly increasing electric field component  $E_{\text{cloud}}$ , with a rise rate lower than 1 KV/m/s (Cooray 2010) i.e., during the inception of stable upward leaders,  $E_{\text{cloud}}$  is considered to be constant because this process has duration of around few hundred microseconds. However, upward leader models are still being investigated.

For upward propagating lightning from wind turbine, as mentioned above, the electric field in the air is near uniform being produced by the cloud and not by a stepped leader. Therefore, for upward leader formation, the strong influence of the stepped leader position is eliminated, and the formation will be dominated by the wind turbine geometry and the electric field distribution.

The charge structure in a thundercloud is usually replicated by three vertical stacked point charges or spherically symmetrical charge volumes. It consists of a vertical tri-pole made from a negative charge and two positive charges. Details of the vertical tri-pole charge used in this work is given in (Godson, Begam et al. 2017).

In order to analyze the maximum electric field strength required for the initiation of upward leaders from wind turbines, the information from the cloud model is combined with the wind turbine model in the simulation. As

illustrated in (Godson, Begam et al. 2017), the vertical tri-pole model is used to create an ambient field representing uniform electric field due to cloud charge distribution at 200m above ground.

The wind turbine model used in this paper is a vesta's wind turbine V100 with 2 MW rated power, 100 m rotor diameter, swept area of 7.854m<sup>2</sup> and a 49 m long blade. V100-2MW is a horizontal axis wind turbine with three blades shown in figure 1 (b). The receptor is integrated into the model design, grounded through the down conductor so as to take the lightning current to ground. Details of the wind turbine and the receptor is given in (Godson, Begam et al. 2017, Godson, Begam et al. 2017).

The model used for rotation evaluation is shown in Figure 1(a). The evaluation is done as the blade is rotated through -60, -55, -50, -45, -40, -35, -30, -25, -20, -15, -10, -5, 0, 5, 10, 15, 20, 25, 30, 35, 40, 45, 50, 55 and 60 degrees from the vertical position. The blade in the vertical position is referred to as blade A and only the results for blade A are provided in this paper. Also, values are obtained from the blade tip, leading edge, trailing edge and the receptor tip. The focus is on characterizing the electric field due to upward initiated lightning by obtaining the maximum electric field strength required for the initiation of upward leader due to thunder cloud charge. The peak current  $I_{peak}$  applied is 30 kA chosen because it represents the general situation of lightning strikes (Ancona and McVeigh 2001).

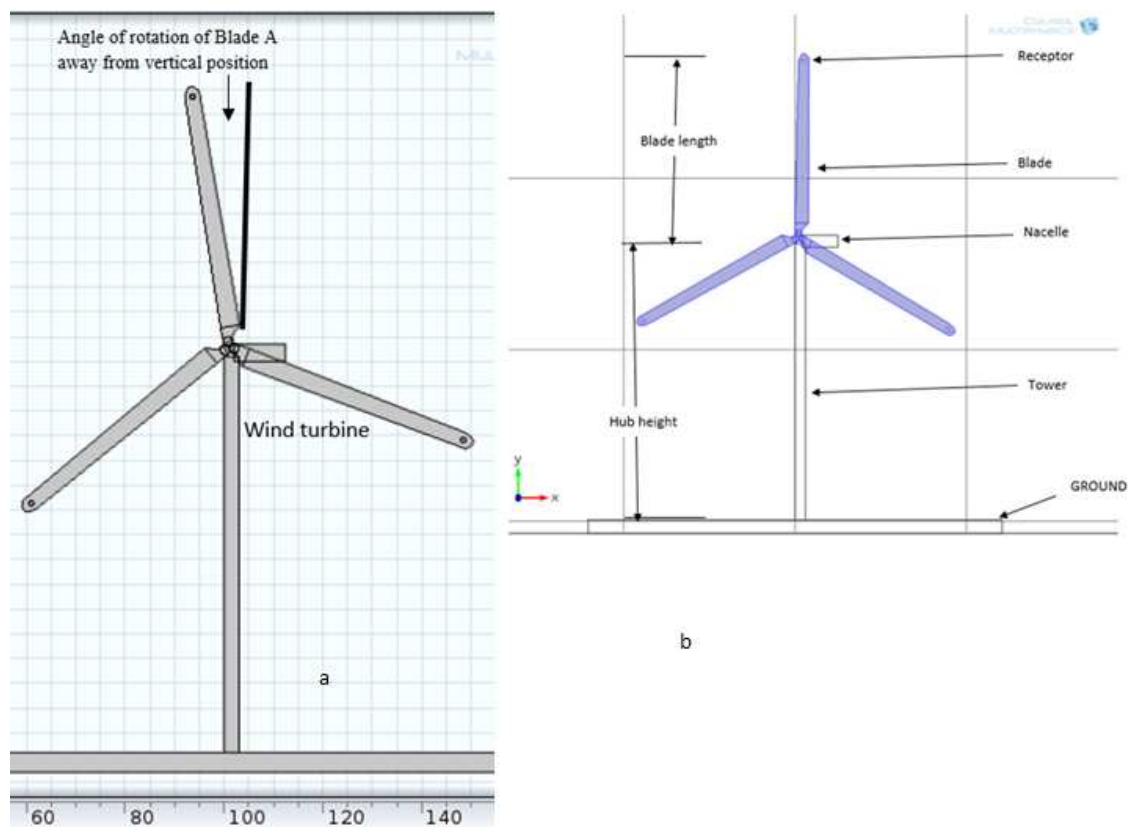


Figure 1. (a) Model used for rotation evaluation. (b) Wind turbine model

The electric field due to thunder cloud charge can be calculated using electrostatics equations. The governing equations are solved with FEA software COMSOL Multiphysics and the computational domain is shown in Figure 1.

### 3. RESULTS AND DISCUSSIONS ON SIMULATION

This section presents the evaluation of the maximum electric field strength on the surface of the blade and on the protection device as the blade is rotated from 0 to 360 degrees. The positions with higher electric field strength are considered to have higher possibility of inception of upward leader. Results are plotted and compared for values obtained from the blade tip, leading edge, trailing edge and the receptor tip. The proficiency of the protection systems depends on the value of the distributed electric field. By comparing the electric field strength as the blade is rotated, the electric field due to upward initiated lightning is characterized.

In order to characterize the electric field due to upward initiated lightning, the simulation is first conducted on the wind turbine without the receptor and then the receptor is applied as the blades are rotated. Figure 2 (a) shows the unprotected wind turbine and Figure 2 (b) presents protected wind turbine while Figure 2 (c) shows the rotated state

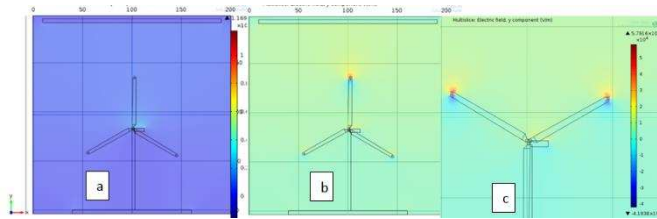
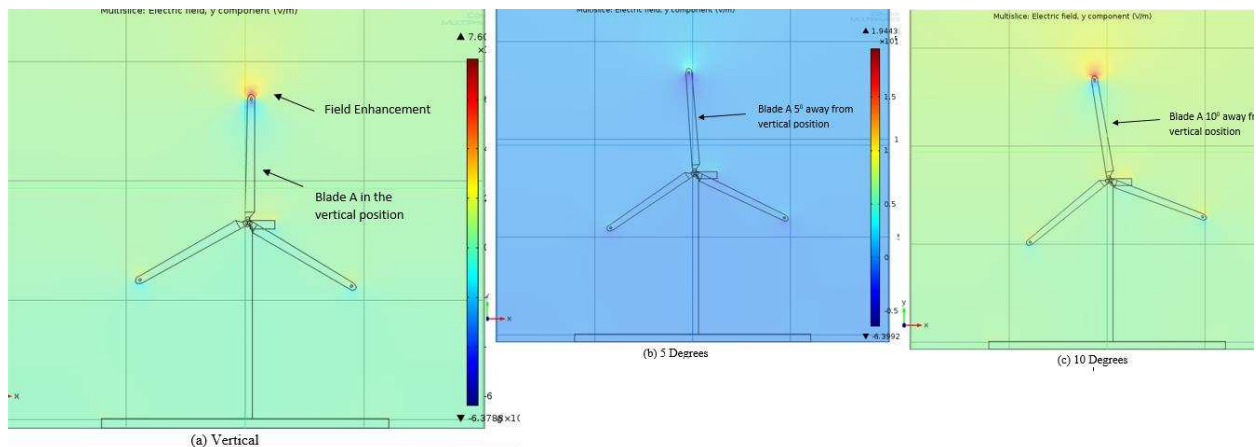
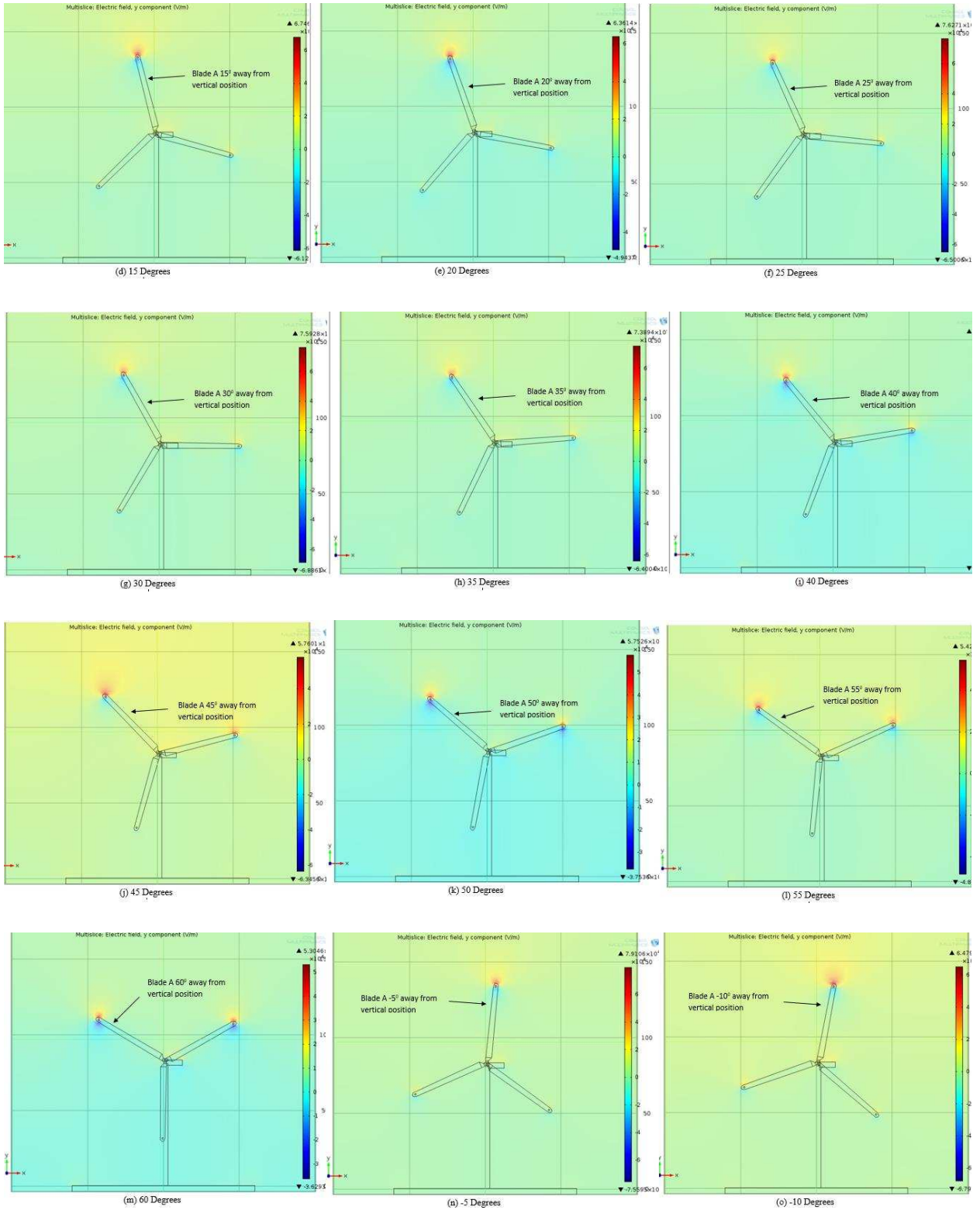


Figure 2. (a) Unprotected wind turbine, (b) Protected and (c) Rotated state (Godson, Begam et al. 2017)

The wind turbine is protected, by activating the receptors, field enhancement is seen as shown above. Details of activities around an activated receptor such as upward positive polarity for streamer activities, the negative polarity going to ground through ground wire, positive polarity on the blade surface and the produced corona charge which lowers the electric field on the tip inhibiting the occurrence of a streamer are shown in (Godson, Begam et al. 2017). Figure 3 shows the maximum electric field distribution due to cloud charge as blade A is rotated from -60 to +60 degrees from the vertical position. These positions are; -60, -55, -50, -45, -40, -35, -30, -25, -20, -15, -10, -5, 0, 5, 10, 15, 20, 25, 30, 35, 40, 45, 50, 55 and 60.





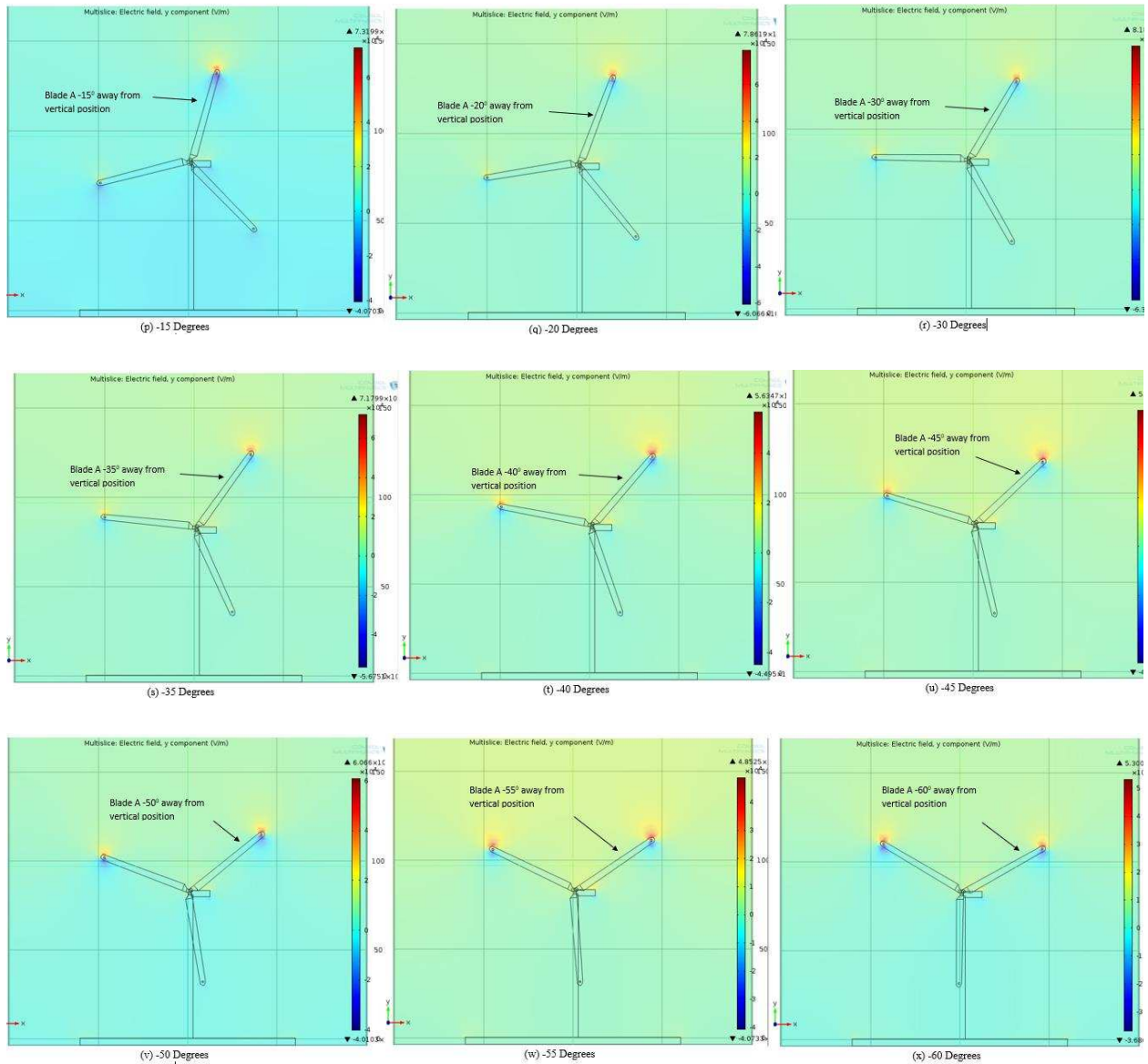


Figure 3. maximum electric field distribution due to cloud charge as blade A is rotated from -60 to +60 degrees from the vertical position.

The plot for -25 degrees is not shown, this is because -25 degrees could not generate a plot perhaps due to mesh. Changing the mesh size at this stage may undermine the result. Consequently, no values are obtained for this position. The results for maximum electric field strength distributions for various configurations obtained from the blade tip, leading edge, trailing edge and the receptor tip, as blade A is rotated are shown in table 1 and plotted in Fig. 4-7.

Table 1 Values for maximum electric field strength (kV/m) obtained.

Angle from vertical	Blade tip	Leading Edge	Trailing Edge	Receptor
-60	19.79	39.80	-0.66	29.28
-50	22.53	41.80	2.86	36.34
-45	26.53	42.91	6.36	42.89

-40	30.78	44.27	8.00	29.16
-35	35.73	44.46	13.49	56.13
-30	38.92	44.44	17.57	65.96
-25	41.93	44.10	21.91	68.67
-20	49.46	41.40	29.85	80.44
-15	54.54	39.89	38.24	82.15
-10	56.70	36.48	40.14	90.46
-5	56.43	29.46	46.81	89.71
0	59.06	20.05	55.61	85.26
5	55.67	15.28	55.51	86.04
10	54.29	11.44	52.95	63.41
15	51.20	5.14	58.70	76.10
20	49.31	1.12	56.95	69.39
25	41.99	-2.33	53.61	66.20
30	37.66	-6.23	50.80	56.87
36	35.94	-9.57	50.82	61.44
40	30.49	-11.67	43.50	43.12
45	26.02	-13.42	40.39	35.38
50	21.33	-14.70	38.75	31.29
60	19.79	39.80	-0.65	29.28

To characterize the distributed electric field and to show the clear difference, both Radar and Area charts are plotted in each case for the Blade Tip, Leading edge, Trailing Edge and the Receptor Tip. The receptor tip refers to the electric field distribution at the upper part of the metallic receptor.

#### A. Blade Tip

The area and radar plots for the electric field distribution on the surface of the blade tip is shown below in Figure 4.

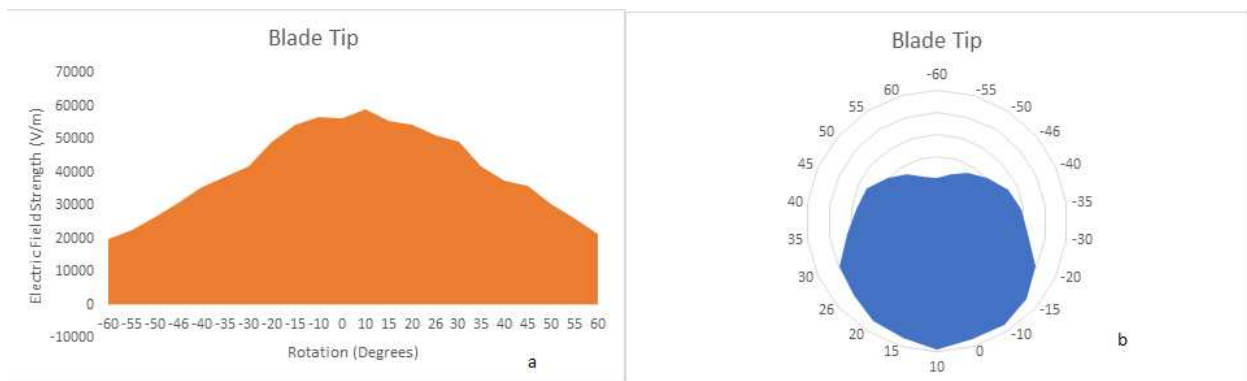


Figure 4. The (a) Area and (b) Radar plots for the electric field distribution on the surface of the blade tip

From the area plot in Figure 4 (a), starting from -60 degrees on the rotation axis, the electric field distribution at the blade tip is minimum (19.79 kV/m) at -60 degrees, increasing slightly uniformly to -10 degrees and then a slight

decrease afterward. The electric field distribution reaches maximum at 10 degrees, after which it decreases slightly uniformly until it reaches 60 degrees.

The radar plot is shown in Figure 4 (b). The electric field distribution on the blade tip due to upward initiated lightning is fairly smooth and point of lightning attachment is easily predicted from the value of the distributed electric field.

### B. Leading Edge

The area and radar plots for the electric field distribution on the surface of the blade leading edge is shown below in Figure 5.

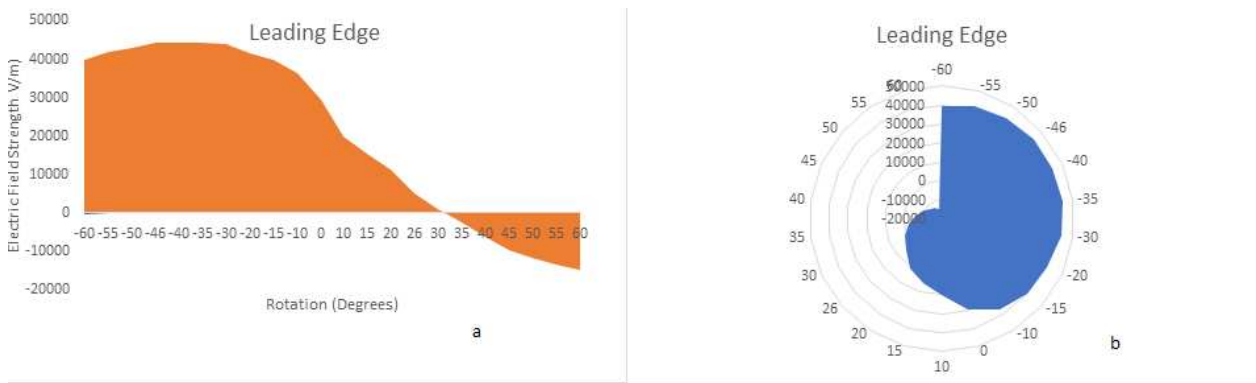


Figure 5. The (a) Area and (b) Radar plots for the electric field distribution on the surface of the blade leading edge

The area plot for the electric field distribution at the blade leading edge is shown above in Figure 5 (a). Starting from -60 degrees, with electric field of (39.80 kV/m), it increased slightly and remained slightly uniform until it begins to decrease at -35 degrees with electric field value of (44.46 kV/m). It finally falls to zero at 30 degrees and beyond.

The radar plot is shown in Figure 5 (b), the electric field distribution on the leading edge due to an upward initiated lightning is fairly smooth though slightly rougher than that of the blade tip and point of lightning attachment can also be easily predicted from the value of the distributed electric field.

### C. Trailing Edge

The area and radar plots for the electric field distribution on the surface of the blade trailing edge is shown below in Figure 6.

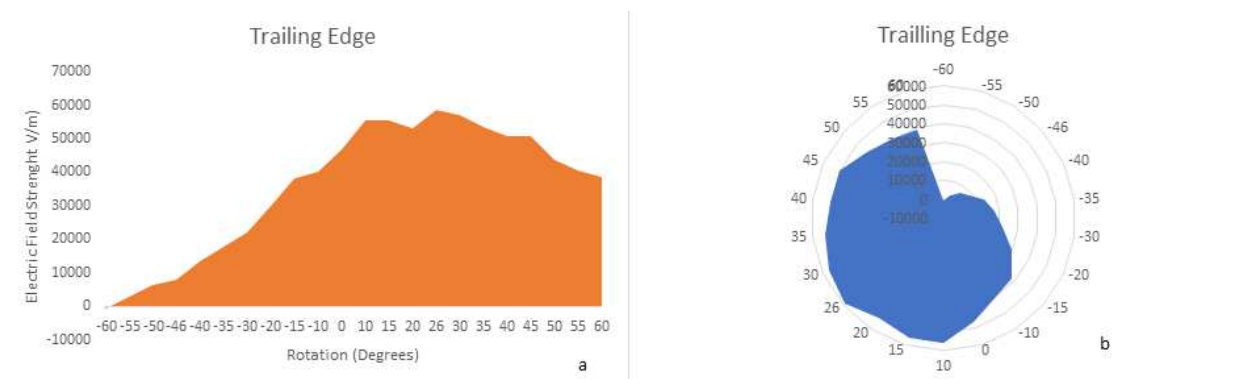


Figure 6. The (a) Area and (b) Radar plots for the electric field distribution on the surface of the blade trailing edge

The electric field distribution on the trailing edge is very rough as shown in the area plot in Figure 6, i.e. it is not as smooth as that on the leading edge. As usual, starting from -60 degrees with minimum electric field distribution below (0 kV/m), increasing slightly uniformly to 0 degrees (55.61 kV/m) and then a slight decrease after which reaches maximum at 15 degrees (58.70 kV/m) and 30 degrees (50.80 kV/m). It then decreases slightly uniformly until 60 degrees.

From the radar plot in Figure 6 (b), the electric field distribution on the trailing edge due to an upward initiated lightning as compared to blade tip and the leading edge is relatively rough and point of lightning attachment can also be predicted from the value of the distributed electric field.

#### D. Receptor Tip

The area and radar plots for the electric field distribution on the surface of the tip of the receptor is shown below in Figure 7.

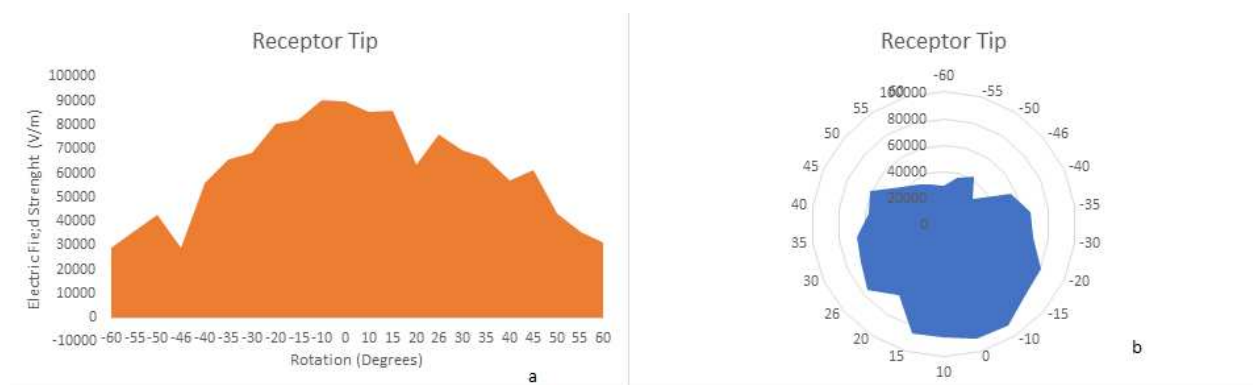


Figure 7. The (a) Area and (b) Radar plots for the electric field distribution on the receptor tip

The electric field distribution on the tip of the receptor is shown in Figure 7 (a) above. These values are obtained from the tip of the receptor (a point on the receptor closest to the blade tip). The plot is rougher than that obtained from the surface of the blade. Starting from -60 degrees, with electric field distribution of (29.28 kV/m), increases uniformly to -45 degrees to (42.89 kV/m), it then drops sharply at -40 degrees to (29.16 kV/m). The electric field distribution then increases slightly uniformly until it gets to maximum at -10 degrees (90.46 kV/m), after which it falls irregularly until 60 degrees (29.28 kV/m).

The radar plot for the electric field distribution on the receptor tip due to upward initiated lightning is shown above in Figure 7 (b). As compared to the blade surface (Blade tip, leading edge and the trailing edge of the blade), the field plot on the receptor tip is characterized by very rough surface and as usual, point of lightning attachment can be predicted from the value of the distributed electric field. The complex nature of the field distribution on the receptor though explains why the receptor is the most attractive point for lightning attachment, however, due to the roughness, it is also possible at some point for the receptor to be less attractive, consequently, lightning will strike other part of the wind turbine instead of the receptor.

## 4. EXPERIMENTAL EVALUATION

This section describes the validation of the simulation model used in characterizing the maximum electric field strength required for the initiation of upward leader from wind turbine. High voltage test is carried out to study the development of streamers. Also, the conductivity of the blade samples is also considered. Obtained experimental results are compared with that of simulation and then discussed.

#### 4.1. Experimental Setup and Procedure for High Voltage Strike Attachment Test

The high voltage strike attachment test is usually applied to determine specific lightning attachment points on a structure. The main idea is to know from where upward initiated leaders or answering leaders are emitted.

The test arrangement is intended to result in initiation of electrical activity, such as corona, streamers and leaders at a wind turbine blade just before a lightning strike attachment. Immediately ionization of the air at the wind turbine blade test specimen is initiated, the inception streamer will progress towards the ground which has a large geometry and is intended to represent an electric field equipotential surface some distance from a blade extremity. In this manner, the influence of the external test electrode on test results is minimized. Figure 9 shows the setup for the test arrangement, this include; high voltage generator, blade test specimen and ground. This test setup is chosen because it usually allows a larger dimension external electrode (i.e. a conductive surface on the floor of the laboratory) and a more realistic electric field environment during the test around the blade specimen to be provided. The test is performed by elevating the specimen above a grounded test plane in a high voltage laboratory. This grounded plane simulates an equipotential plane of the electric field between the blade tip and an approaching lightning leader of a downward initiated lightning flash or the static background electric field present prior to an upward initiated lightning flash.

There are a number of lightning protection methods used on wind turbines, these includes; Receptors, Metallic Cap, Metallic Conductor on the Blade Tip, Mesh, Ring Electrode (Zavareh 2012) and the Backside Electrode (Minowa, Sumi et al. 2012) methods, also the combined cap and receptors method recommended in (Ikhazuangbe, Begam et al. 2019) for offshore wind turbines. However, modern onshore wind turbines are predominantly protected with the receptor method. More also, multiple receptors on the blade has been a focus of research but the single tip receptor method has remained the preferred choice. Therefore, only the single tip receptor method is considered in this experiment.

The receptor though effective (Shindo, Asakawa et al. 2011), also failed in so many instances as mentioned in (Yoh and Shigeru 2011, Yokoyama 2011). The efficiency of the receptor is dependent on its interception proficiency which is its ability to intercept a lightning stroke. This strongly dependent on the characteristics of the electric field distribution.

The test aims at characterizing the electric field distribution due to upward initiated lightning achieved by the value of the distributed electric field and to determine to which point lightning discharge will attach on the wind turbine blade. The test environment experienced by the wind turbine blade is similar to real lightning situation and the entire blade is totally affected by the external field prior to a lightning strike.

The high voltage waveform used is a double exponential switching type impulse voltage with rise times in order of 50-250 $\mu$ s and decay times of 2000 $\mu$ s. This voltage waveform is selected since it is the most representative of the electric field in the vicinity of a structure during an initial leader attachment.

#### 4.2. Test Specimen

In order to assess the normal distribution of the points of discharge attachment on the blade surface, a large sized wind turbine hit by natural lightning strike is experimentally required while it is rotating, this can only be done in the natural lightning laboratory such as in Florida. The protection evaluation is done using 3 m blade tip section that is a part of Vestas V100 wind turbine, with 2 MW rated power, 100 m rotor diameter and 49 m long blade made of glass fibers reinforced polyester, cut from an actual blade. This size is adopted because most of the lightning attachments are located in the tip area of the blade. As compared to full scale wind turbine, testing with small specimens like 3 m of a full-scale length makes it possible to perform many tests within a limited amount of time and the duration for the test in this experiment is within one week. The elevated blade specimen is connected to the output of a Marx generator injecting high voltage impulses into the lightning protection system (receptor) of the blade. Blade thickness is 10 cm, chamber length: 0.9 m, maximum chord 3.9 m. The blades are rotated from 0 to 360 degrees and used to investigate the characteristics of the distributed electric field around an operational wind turbine. The receptor is placed 1.5 m (Godson, Begam et al. 2017) from the blade tip.

During the experiment, the applied receptor is connected to ground through a down conductor of 6 mm<sup>2</sup> cross section area embedded in the blade. A receptor fixed in a blade tip is shown in Figure 8 below.

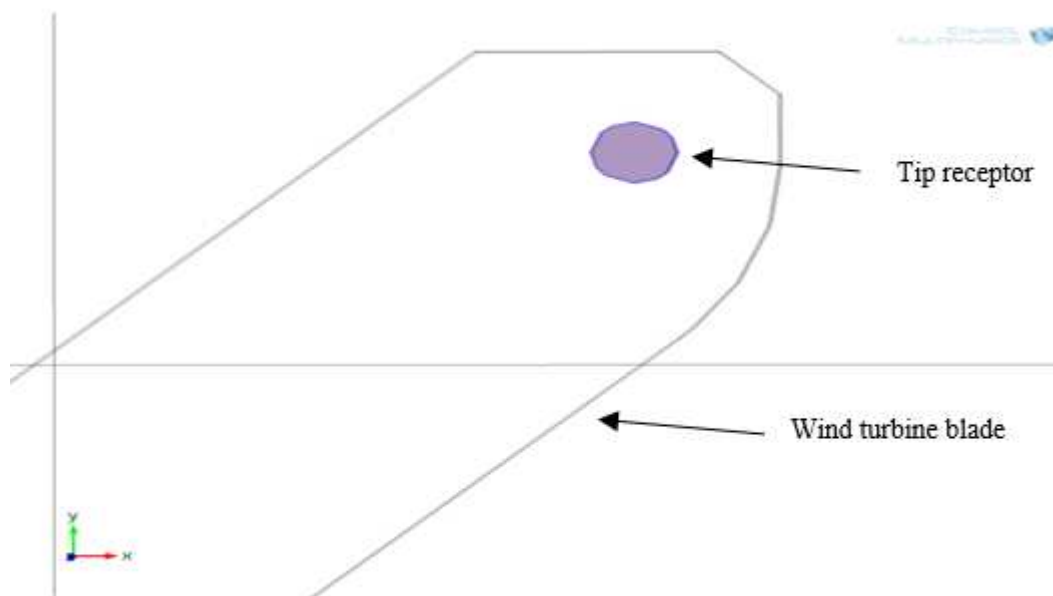


Figure 8. A receptor fixed in a blade tip

### 4.3. Test Setup

The tests are performed on the test setups illustrated in Figure 9 having the blade specimen elevated above a ground plane in the high voltage laboratory.

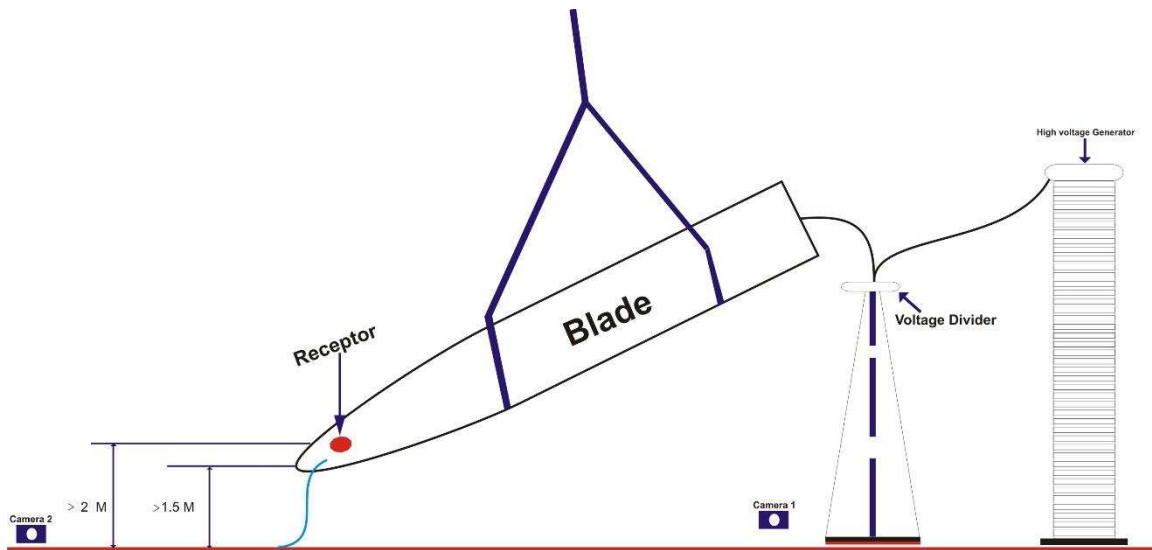


Figure 9. Initial leader attachment test setup

It includes the following:

1. The blade sample described above,
2. Marx generator with resistances and capacitances configured to generate desired voltage waveform.
3. Voltage divider and additional measuring system
4. Digital camera used to determine and show the discharge attachment point to the blade sample.

The size of the ground plane below the blade tip is large enough to avoid discharges from the blade to the edges of the ground plane.

### 4.4. Test Procedure

The Marx generator is adjusted to produce double exponential voltage waveforms D with positive and negative polarity. The blade is then suspended above the ground plane with all distances as shown in figure 9. The output of the Marx generator is connected to the down conductor inside the blade sample and the down conductor is then connected to the lightning receptor.

Five pulses are first applied to the model blade without receptor, then the receptor is applied, and the blade is rotated from 0 to 360 degrees, picture is taken at each discharge. High voltage strike attachment test is performed with the test specimen blade positioned in different orientations as prescribed by IEC 61400-24. In each orientation, the position of the blade is changed as well as the conductivity of the blade and the steps are repeated. Polluted blade surface was achieved with salt contamination 10 g/l solution of sodium chloride (NaCl) sprayed on the surface of the blade. The waveform for each discharge was recorded and, in each case, the peak value and the time to flashover was determined. Determination of the attachment points was made possible by capturing images of the discharge with a digital camera.

As the blade rotates, it was tested, and special attention was given to selected five positions which are pertinent to investigate the performance of wind turbine lightning protection systems on initiation of upward leader. These positions are shown in Figure 10. They are; (b) vertical, (c) 45° (Trailing edge facing the cloud) (TEFC), (d) 45° (Leading edge facing the cloud) (LEFC), (e) horizontal (Trailing edge facing the cloud) (TEFC), and (f) horizontal (Leading edge facing the cloud) (LEFC).

In the experimental configuration, compared to the simulation, the blade in the vertical position referred to as facing the cloud is pointing directly downwards towards the ground plane, where after the tip was pitched in steps of 45°. Also referred to as 45°, Leading or Trailing edge facing the cloud.

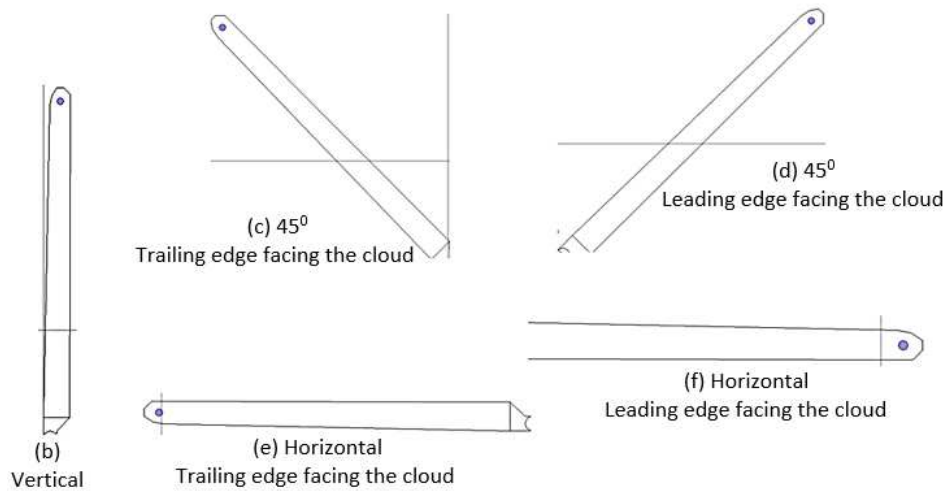


Figure 10. (b, c, d, e and f) Arrangement of blade sample

A 3 m GFRP blade tip elevated above the ground electrode in a laboratory is shown Figure 11.

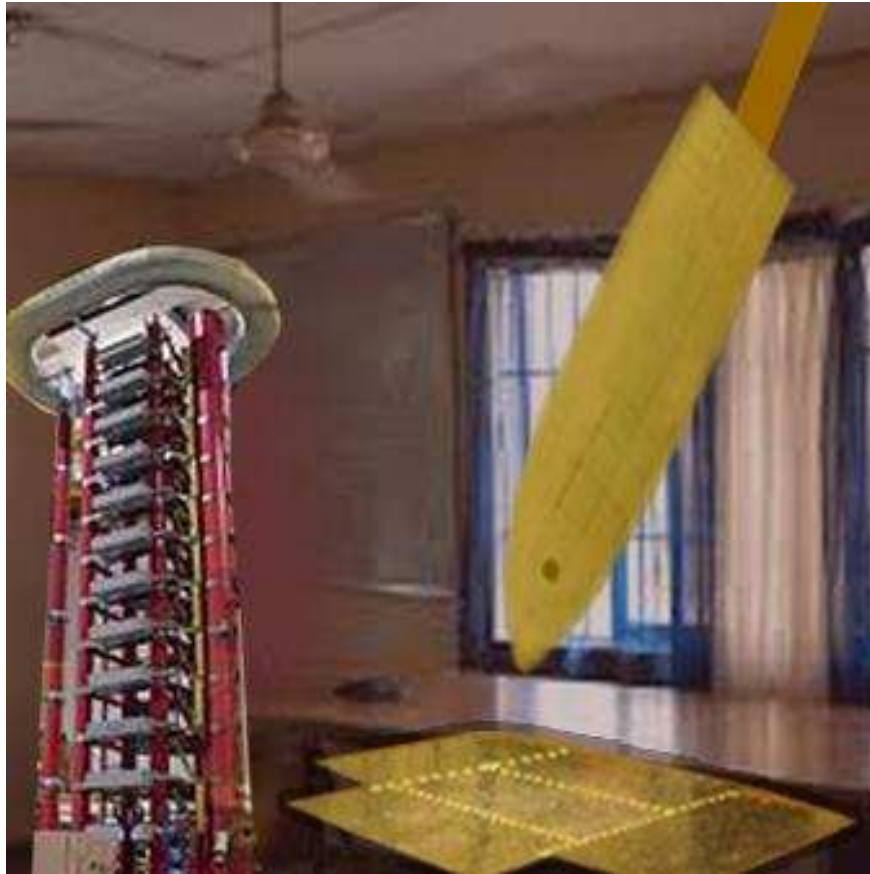


Figure 11. A 3m GFRP blade tip elevated above the ground electrode.

#### 4.5. Experimental Conditions

The protected blade tip was tested as the blade position was changed and the test conducted according to IEC 61400-24. The experiments were performed with the model blade set as a high-voltage electrode. The receptor is a disk-type with a metal disk of size in mm diameter, it is covered with a flat metal braid set on the surface of the modal blade. The polarity of the applied voltage is positive and negative.

The polarity of the charge removed from the thundercloud can be used to sub-divide lightning into negative and positive flashes

A negative flash results in negative charge being transferred to the earth from the thundercloud. They are the dominant type of lightning flashes, around 90% of all cloud to ground, exhibiting the steepest current impulses (highest  $di/dt$ ).

A positive flash lowers positive charge from the thundercloud to the earth, around 10 % of all cloud to ground flashes, exhibiting the most powerful current parameters (higher I, Q and W/R).

The experimental results follow a regular pattern for both positive and negative polarity and are similar to that in literature, however, since negative flashes are the dominant type of lightning and are more pertinent to the present experiment, only results for negative polarity are presented.

## 5. RESULTS AND DISCUSSION ON EXPERIMENTAL EVALUATION

### 5.1. Experiments with and without Receptor on the Model Blade

The test results are summarized as follows.

#### (1) Experiments without receptor on the model blade

Without the receptor, discharge to the model blade occurred at different points.

#### (2) Experiments with receptor on the model blade

The experimental results are shown in Table 2. The results are summarized as follows.

- a. For blade tip facing the ground (Also referred to as vertical position in Figure 10), whether polluted or unpolluted, 100% of the discharge initiated from the receptor.
- b. In the case of 45° (Trailing edge facing the cloud) (TEFC), 95% of the discharge initiated from the receptor, however, 5% of the discharge initiated from the blade trailing edge and was more for the polluted blade condition.
- c. In the case of 45° (Leading edge facing the cloud) (LEFC), 98% of the discharge initiated from the receptor, and 2% of the discharge initiated from the blade leading edge and was also more for the polluted blade condition.
- d. In the case of horizontal (Trailing edge facing the cloud) (TEFC), the observation was similar to (b) above.
- e. In the case of horizontal (Leading edge facing the cloud) (LEFC), the receptor performance at this position was relatively better, 99% of the discharge initiated from the receptor.

Other forms of discharge were also observed, puncture discharges from inside the blade sample to the ground occurred. In some cases, discharge incepted from a receptor progressed on the blade surface and then terminated to the ground. Image of a negative discharge terminating on the ground is shown in Figure 12.



Figure 12. discharge from the blade tip towards the ground plane.

Table 2. No of discharge initiation for a blade-to-ground gap

Blade tip angle from ground plane	Blade tip	Leading Edge	Trailing Edge	Receptor
$-90^0$	1	1	0	18
$-45^0$	1	1	0	18
$0^0$	0	0	0	20
$45^0$	2	0	2	16
$90^0$	1	0	2	17

Different blade configurations were tested. Depending on the blade position, the discharge initiation behaved differently. An efficient protection system against upward initiated lightning can better influence initiation of discharge from the protection device itself rather than the blade surface. This is necessary for a more efficient lightning protection. Occasionally, discharge is initiated from the blade surface rather than the receptor, in this case, failure of receptor is discussed and determined. The points of discharge initiation correlated very well with experience with wind turbine blades in service that have been struck by lightning.

To pass the test by a receptor, all or majority of the discharge must initiate from the receptor. To fail, all or majority of the discharge have to initiate from the blade surface or other part of the wind turbine.

The maximum electric field strength on the model shown in Figure 3 with blade A at the vertical position is located between the receptor and the blade tip, which indicates that an upward leader will likely be initiated from that position. This agrees favorably well with the number of discharge initiation at this position in the experimental result indicating that the tip is worst hit. In addition, the figure reveals that the maximum electric field strengths locations are changing as the wind turbine is rotating. This is also in line with the number of discharge initiation indicating that the blade position affects the lightning attachment manner as well as the performance of the blade lightning protection systems. Another very important correlation of the simulation with experimental result is that in most cases in the simulation, the maximum electric field strength locations on the trailing edge are higher than that on the leading edge which agrees with experimental result in which the blade trailing edge has discharges more times than the blade leading edge. The implications of these two correlations are that as the blade is rotated, the points of leader inception changes and it is likely going to be more at the trailing edge than at the leading edge.

Experimental results for both polluted and unpolluted blade conditions show that the receptor performed better in the case of unpolluted blade surface than the case of the polluted blade surface.

## 6. CONCLUSION

The blades of a modern sized wind turbine are rotated from 0 to 360 degrees and used to investigate the characteristics of the distributed electric field around an operational wind turbine using finite element analysis and the results are supported by experimental evaluation.

The waveforms for the electric field distribution on the blade tip, Blade leading edge, Blade trailing edge and the receptor used for the protection of a wind turbine from lightning are presented.

The electric field distribution is found to be different from that generated by a stepped leader in downward initiated lightning and could seriously influence the lightning protection systems.

The Area and Radar plot showed that the electric field distribution on the blade tip due to an upward initiated lightning is fairly smooth and point of lightning attachment is easily predicted from the value of the distributed electric field.

The electric field distribution on the leading edge due to an upward initiated lightning is found to be fairly smooth though slightly rougher than that of the blade tip.

The electric field distribution on the trailing edge due to an upward initiated lightning as compared to blade tip and the leading edge is relatively rough. i.e. it is not as smooth as that on the leading edge indicating that leader would initiate more from the trailing edge than the leading edge.

The electric field distribution on the receptor tip due to an upward initiated lightning as compared to the blade surface (Blade tip, leading edge and the trailing edge of the blade), the field plot on the receptor tip is characterized by very rough surface. The complex nature of the field distribution on the receptor though explains why the receptor is the most attractive point for lightning attachment, however, due to the roughness, it is also possible at some point for the receptor to be less attractive, consequently, lightning will strike other part of the wind turbine instead of the receptor. Conclusively, the field around the blade surface and the receptor for an upward initiated lightning is more complex than was assumed and different from downward initiated lightning. Existing lightning protection devices originally designed for downward initiated lightning will not be able to work satisfactorily with these complex electric field due to upward initiated lightning, as a result, modern wind turbines due to their heights are at higher risk of failures of their protection devices.

Vulnerable points for lightning attachments can be predicted from the electric field distribution. The electric field characteristics is very useful for the lightning protection engineer designing lightning protection system.

## REFERENCES

Ancona, D. and J. McVeigh (2001). "Wind turbine-materials and manufacturing fact sheet." Princeton Energy Resources International, LLC **19**.

Becerra, M. and V. Cooray (2006). "A self-consistent upward leader propagation model." Journal of Physics D: Applied Physics **39**(16): 3708.

Becerra, M. and V. Cooray (2008). "On the velocity of positive connecting leaders associated with negative downward lightning leaders." Geophysical Research Letters **35**(2).

Byrne, A. and M. Malkin "Field Performance Assessment of Wind Turbine Lightning Protection Systems."

Cooray, V. (2010). "Lightning protection. The Institution of engineering and technology." London: The Institution of Engineering and Technology.

Diendorfer, G. (2010). "LLS performance validation using lightning to towers." Impulse 1(7.5): 11.

Diendorfer, G. (2011). Lightning initiated from tall structures—A review. Lightning Protection (XI SIPDA), 2011 International Symposium on, IEEE.

Diendorfer, G. (2015). On the risk of upward lightning initiated from wind turbines. Environment and Electrical Engineering (EEEIC), 2015 IEEE 15th International Conference on, IEEE.

Diendorfer, G., et al. (2009). "Some parameters of negative upward-initiated lightning to the Gaisberg tower (2000–2007)." IEEE Transactions on Electromagnetic Compatibility 51(3): 443-452.

Diendorfer, G., et al. (2011). Review of 10 years of lightning measurement at the Gaisberg Tower in Austria. Proc. 3rd International Symposium on Winter Lightning, Sapporo, Japan.

Godson, I., et al. (2017). "Optimum receptor location for efficient lightning protection of modern wind turbines." International Journal of Simulation Systems, Science & Technology 18.

Godson, I., et al. (2017). "Receptor Sizes and Its Effect on Lightning Protection of Modern Wind Turbines." Journal of Green Engineering 7.

Guimarães, M., et al. (2014). "Assessing currents of upward lightning measured in tropical regions." Atmospheric Research.

Ikhazuangbe, G., et al. (2019). "Effect Of Pollution On Offshore Wind Turbine Blade Lightning Protection Systems.pdf." Journal of Multidisciplinary Engineering Science and Technology 6(4).

Ikhazuangbe, G., et al. (2019). Performance Enhancement of Lightning Protection Systems for Offshore Wind Turbine Blades. International Symposium on Lightning Protection (XV SIPDA), São Paulo, Brazil.

Ikhazuangbe, G. I., et al. (2019). Testing of Wind Turbine Lightning Protection Systems – Comparison of Testing the Full-Scale Blade Length and a Small Section of the Blade Tip. International Symposium on Lightning Protection (XV SIPDA). São Paulo, Brazil.

Lu, W., et al. (2009). "Two associated upward lightning flashes that produced opposite polarity electric field changes." Geophysical Research Letters **36**(5).

Lyons, W. A., et al. "Meteorological Aspects of Two Modes of Lightning-Triggered Upward Lightning (LTUL) Events in Sprite-Producing MCS."

Miki, M., et al. (2005). "Initial stage in lightning initiated from tall objects and in rocket-triggered lightning." Journal of Geophysical Research: Atmospheres **110**(D2).

Minowa, M., et al. (2012). A study of lightning protection for wind turbine blade by using creeping discharge characteristics. Lightning Protection (ICLP), 2012 International Conference on, IEEE.

Montanyà, J., et al. (2014). "Lightning discharges produced by wind turbines." Journal of Geophysical Research: Atmospheres.

Peesapati, V. and I. Cotton (2009). Lightning protection of wind turbines—A comparison of real lightning strike data and finite element lightning attachment analysis. Sustainable Power Generation and Supply, 2009. SUPERGEN'09. International Conference on, IEEE.

Rachidi, F., et al. (2008). "A review of current issues in lightning protection of new-generation wind-turbine blades." Industrial Electronics, IEEE Transactions on **55**(6): 2489-2496.

Shindo, T., et al. (2011). "Characteristics of lightning strikes on wind turbine blades. Experimental study of the effects of receptor configuration and other parameters." Electrical Engineering in Japan **176**(3): 8-18.

Wang, D., et al. (2008). "Observed characteristics of upward leaders that are initiated from a windmill and its lightning protection tower." Geophysical Research Letters **35**(2).

Yoh, Y. and Y. Shigeru (2011). Proposal of lightning damage classification to wind turbine blades. Lightning (APL), 2011 7th Asia-Pacific International Conference on, IEEE.

Yokoyama, S. (2011). Lightning protection of wind turbine generation systems. Lightning (APL), 2011 7th Asia-Pacific International Conference on, IEEE.

Zavareh, H. T. (2012). Wind turbines protection against the lightning struck using a combined method. Renewable Energy and Distributed Generation (ICREDG), 2012 Second Iranian Conference on, IEEE.

Zhou, H., et al. (2012). "Measured current and close electric field changes associated with the initiation of upward lightning from a tall tower." Journal of Geophysical Research: Atmospheres **117**(D8).

